'88 KACC 1988.10.21~22

Development of a Fully Integrated Simulation Package for Industrial Robot

°Min Ki Lee, Gwang Nam Lee, and Kye Young Lim

Goldstar Industrial System Co., Ltd.

Lucky-Goldstar R & D Complex

ABSTRACT

The purpose of this paper is the development of a fully integrated simulation package for industrial robot. The simulation package consists of kinematics, dynamics, and control. The kinematics contains trajectory plans and inverse kinematics. The dynamics combines manipulator dynamics and actuator dynamics including the effect of payloads and viscous frictions. The control is a hardware oriented scheme which contains position controller, velocity controller, current controller, and PWM generator. Thus, the simulation package can be used not only for theoretical purposes but also for development purposes in industry. Using this package, the characteristics and performances of the SCARA robot, which has been developed in GSIS, are investigated.

I. Introduction

The simulation package provides the information of robot dynamics for various motion plans and manipulator structures. This information is useful for the selection of actuators and the design of the manipulators. A large number of simulation packages have been developed for the purpose of the varification of control algorithms. When a control algorithm is applied to a robot, the simulation package is used to analyze its performance. However, most of the packages are formulated on the basis of the manipulator dynamics only [1,2]. The control input is the required joint torque or force to maintain the desired motion of the manipulator. In practice, this input can not directly be applied to the robot since the robot control input is not the torque or force but the voltage supplied to the actuator [3,4]. Furthermore, the algorithm computes the control inputs based on the manipulator dynamics even though the performance of the robot is strongly affected by the actuator.

In this paper, an integrated simulation package is developed for the industrial robot. The package is used to design and develop a SCARA robot. The SCARA has been developed in the GSIS as an assembly robot with high speed and high accuracy. It uses a DC servo motor as the actuator whose dynamics is included in the dynamic model in combination with the manipulator dynamics. With the integrated dynamic model, the control can deal with the effects caused by the actuator. Viscous frictions are also included in the dynamic model and their coefficients are updated by Lagrangian polynomial method according to the joint speeds. The control scheme of the simulation package is the same as that of the SCARA. The control input is the voltage supplied to the DC servo motor. The voltage is determined through postion, velocity, and current controllers and modulated as a pulse width by the PWM generator.

II. SCARA Robot

2.1 Manipulator

As shown in Figure 1, the SCARA is an open-loop type manipulator composed of A, B, Z, and W axes. The A and B axes are actuated by the DC servo motors through harmonic drives whose backlashes do not almost exist. These axes yield the horizontal motion of the robot arm within the work space. The Z axis is moved up and down by a ball screw which converts the rotational motion of the motor to the translational motion of the axis. This axis generates the vertical motion of the robot end-effector. Finally, the rotation of the end-effector is monitored by W axis which is driven by the DC servo motor through a gear box.

The motion of the manipulator is described by kinematics [5]. It is the expression for the end-effector frame relative to the base frame. That is,

$$ {}^{0}_{4}A = {}^{0}_{1}A\,{}^{1}_{2}A\,{}^{2}_{3}A\,{}^{3}_{4}A = \left[\begin{array}{c|c} {}^{0}_{4}R & \begin{matrix} P_x \\ P_y \\ P_z \end{matrix} \\ \hline 0 \quad 0 \quad 0 & 1 \end{array}\right] \qquad (1) $$

where,

$$ {}^{0}_{4}R = \begin{bmatrix} -\sin(\theta_1+\theta_2+\theta_4) & -\cos(\theta_1+\theta_2+\theta_4) & 0 \\ \cos(\theta_1+\theta_2+\theta_4) & -\sin(\theta_1+\theta_2+\theta_4) & 0 \\ 0 \quad 0 & 0 & 1 \end{bmatrix} \qquad (2) $$

$$ \begin{aligned} P_x &= a_1\cos\theta_1 + a_2\cos(\theta_1+\theta_2) \\ P_y &= a_1\sin\theta_1 + a_2\sin(\theta_1+\theta_2) \\ P_z &= -d_2 - d_3 \end{aligned} \qquad (3) $$

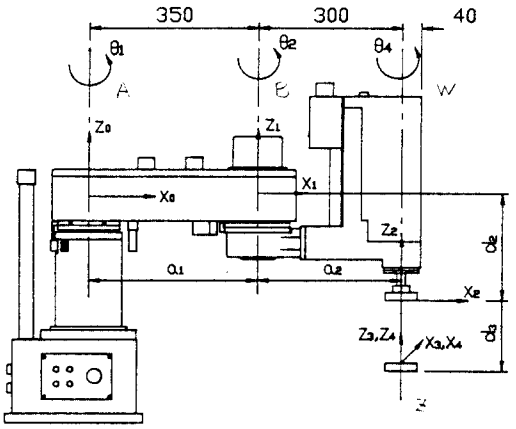

Figure 1. SCARA Manupulator

Based on this analytical expression, the inverse kinematics is solved by closed form solutions;

Let $r^2 = P_x^2 + P_y^2$

$A = (r^2 - a_2^2 - a_1^2) / 2a_1 a_2$

$$\Theta_2 = \tan^{-1}\left[\pm \sqrt{1-A} / A\right] \quad (4)$$

$$\Theta_1 = \tan^{-1}[P_y / P_x] + \tan^{-1}[a_1 \sin\Theta_2 / (a_1 \cos\Theta_2 + a_2)] - \Theta_2 \quad (5)$$

$$d_3 = -d_2 - P_z \quad (6)$$

2.2 Controller

The SCARA control scheme consists of three major parts; main controller, axis controller, and servo driver as shown in Figure 2.

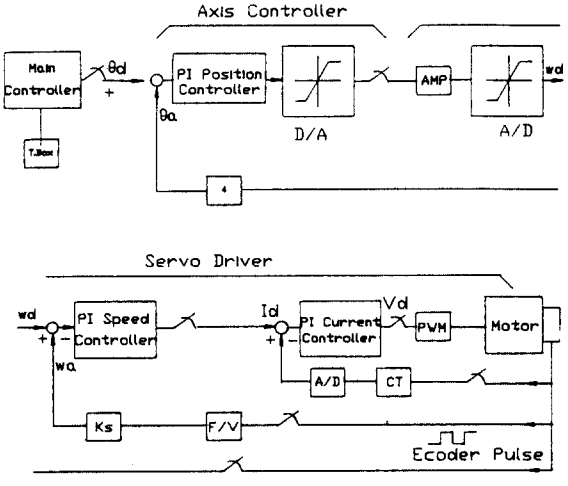

Figure 2. SCARA Control Scheme

A. Main Controller

The main controller is interfaced with a teaching box. With this box, an operator teaches the points that the robot will move. Given the teaching points, the main controller generates a smooth velocity curve and integrates it to provide desired positions [6]. The controller can generate linear and circular motions as well as point to point motions. The inverse kinematics is conducted to compute the set of joint positions for the linear and circular motions. The desired joint positions are converted into the number of encoder pulses. In order to increase a position resolution, the number of pulses is multiplied by four and then it becomes the desired position commend.

B. Axis Controller

The purpose of the axis controller is positioning of motor shaft to the desired position. An encoder is attached to each motor shaft. It detects the actual position of the motor and generates the corresponding number of pulses. Each pulse is reformed to be four up or down pulses.

The axis compares the desired position command from the main controller with the actual position commend from the encoder to find the position error. It goes through PI position controller and D/A converter to generate the velocity command. It is proportional to a desired motor velocity, and is scaled such that ± 8 V corresponds to the maximum motor speed in both CW and CCW directions.

C. Servo Driver

The servo driver consists of speed controller, current controller, and PWM generator. The velocity command is sent to the servo driver and is converted to the digital signal through A/D. The driver senses the motor speed by counting the number of the encoder pulses during a fixed time interval. The PI speed controller computes the desired current input, Id, based on the desired and actual velocities. The Id is now sent to a current controller which generates the desired voltage, Vd, in the same way of the speed controller. Finally, this desired voltage is sent to the PWM generator which modulates the pulse width as shown in Figure 3 [7].

The Vd is the constant voltage for the sampling time and the voltage pulse width plays the role of the input for a motor controlled. The pulse width is determined by comparing the desired voltage with the referrence triangular wave. According to the pulse width, the PWM circuit switches either on or off the power-output transistors which connect the motor in a "H-bridge" configuration.

III. Dynamic Model

3.1 Manipulator Dynamics

The dynamic behavior of a robot manipulator is described by differential equations. These equations

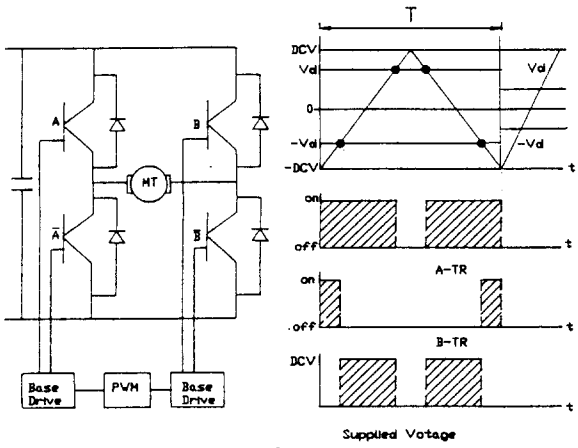

Figure 3. PWM Generator

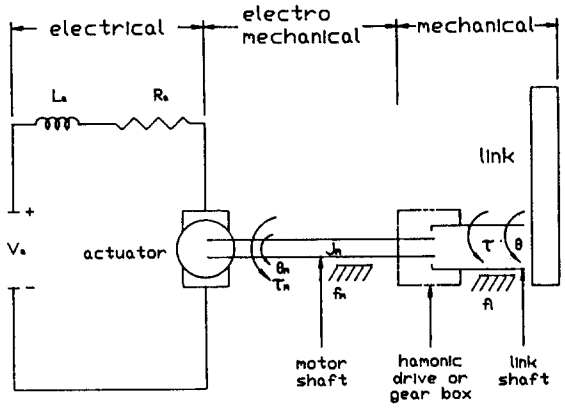

Figure 4. Actuator-Gear-Link Assembly

relate the joint forces or torques exerted by the actuators to the manipulator's dynamics. Lagrangian formulation is applied to derive the dynamic equations of the motion of the manipulator [8]. The formulation represents the dynamics of rigid bodies, and it has the form;

$$\frac{d}{dt}\frac{\partial L}{\partial \dot{q}_i} - \frac{\partial L}{\partial q_i} = Tl_i \qquad i = 1, 2, \ldots, n \qquad (7)$$

Where q_i = generalized coordinate representing the displacement of joint i,
L = kinetic energy − potential energy , and
Tli = generalized force acting on the joint.

When the formulation is applied to the SCARA manipulator with n=4, the manipulator's dynamics is expressed in a compact form;

$$Tl = D(\Theta)\ddot{\Theta} + H(\Theta,\dot{\Theta}) + G(\Theta) \qquad (8)$$

Where $Tl = [\tau_1\ \tau_2\ f_3\ \tau_4]^T$,

$D(\Theta)$ = 4 X 4 inertia matrix,

$H(\Theta,\dot{\Theta})$ = 4 X 1 Coriolis and centrifugal force matrix, and

$G(\Theta)$ = 4 X 1 gravity force matrix.

3.2 Integrated Dynamic Model

The actuator dynamics is combined with manipulator dynamics to formulate the integrated dynamic model. As shown in Figure 4, the actuator-gear-link assembly can be considered as three major parts; electrical, electromechanical, and mechanical.The dynamic equations for these three parts are as follows:

A) Electrical Part

By applying the Kirchhoff's voltage law to the armature circuit, one obtains

$$Va(t) = Ra\ Ia(t) + La\frac{d\ Ia(t)}{d\ t} + Vb(t) \qquad (9)$$

where Va = voltage in volt,
Ra = resistance in Ω,
Ia = current in ampere,
La = inductance in henry, and
Vb(t) is the back electromotive force (emf) in the armature winding which can be represented by

$$Vb(t) = Kb\ \dot{\Theta}m\ (t) \qquad (10)$$

where Kb = proportional constant,

$\dot{\Theta}m(t)$ = angular velocity of the motor shaft.

B) Electromechanical Part

The DC motor is operated in its linear range so that the generated torque is proportional to the armature current;

$$\tau m = Kt\ \ Ia(t) \qquad (11)$$

Where τm = motor torque,
Kt = motor torque proportional constant.

C) Mechanical Part

The motor shaft is mechanically connected to an actuator-gear-link assembly. As shown in Figure 4, the motor torque τm must be equal to the torque required to overcome the inertia, the viscous friction, and the load torque referred to the motor shaft. That is,

$$\tau m = Jm\ \ddot{\Theta}m + fm\ \dot{\Theta}m + fl/n^2\ \dot{\Theta}m + \tau/n \qquad (12)$$

where Jm = motor inertia,
fm = motor viscous friction coefficient,
fl = load viscous friction coefficient,
τ = load torque referred to the link shaft, and
n = $\Theta m/\Theta$; gear reduction between motor shaft and link shaft.

The τ is the joint torque of the manipulator obtained from the equation 8. The fm and fl are changed as a function of velocities so that they are updated by Lagrangian polynomial [9]. In the equation, the loads refered to the link shaft is converted into the loads referred to the motor shaft through the gear reduction (i.e., $\tau \rightarrow \tau/n$ and $fl\,\dot{\Theta} \rightarrow fl/n^2\,\dot{\Theta}m$). The above combined dynamics is now expressed in terms of the torques acting on the motor shaft;

$$\tau m = De(\Theta)\,\ddot{\Theta}m + Fe\,\dot{\Theta}m + Td \qquad (13)$$

where $De(\Theta) = Jm + D(\Theta)/N^2$,

$N = \mathrm{diag}\,[n_1\ n_2\ n_3\ n_4]$,

$Fe = fm + fl/N^2$, and

$Td = [H(\Theta,\dot{\Theta}) + G(\Theta)]/N$.

These equations of the motion represent the dynamic model on the actuator space combining actuator dynamics and manipulator dynamics.

IV. Development of a Simulator

A simulator is used to compute how a robot will move under the application of the control inputs. The simulator is developed by reforming the integrated dynamic model. From the equation 13, the acceleration is computed as a function of the motor torque;

$$\ddot{\Theta}m = De(\Theta)^{-1}\,(\tau m - Td - Fe\,\dot{\Theta}m) \qquad (14)$$

The $De(\Theta)^{-1}$ exists since $De(\Theta)$ is always a symmetric and positive definite matrix. Once the acceleration is computed, state equations are developed and integrated to find velocity and position. They are

$$\frac{d\,Ia}{dt} = -Ra/La\ Ia - Kv/La\ \dot{\Theta}m + Va/La \qquad (15)$$

$$\frac{d\,\Theta m}{dt} = \dot{\Theta}m \qquad (16)$$

$$\frac{d\,\dot{\Theta}m}{dt} = De(\Theta)^{-1}\,[Kt\ Ia - Td - Fe\,\dot{\Theta}m] \qquad (17)$$

Let $Y = [Y_1\ \ Y_2\ \ Y_3] = [Ia\ \ \Theta m\ \ \dot{\Theta}m]$

from the state equations,

$$\dot{Y} = \begin{bmatrix} \dot{Y}_1 \\ \dot{Y}_2 \\ \dot{Y}_3 \end{bmatrix} = \begin{bmatrix} (Va - Kv\,Y_3 - Ra\,Y_1)/La \\ Y_3 \\ De(Y_2/n)^{-1}\,[Kt\,Y_1 - Fe\,Y_3 - Td] \end{bmatrix} = F(Y,Va) \qquad (18)$$

Given the current state Y(k) and input voltage Va(k), the next state Y(k+1) is solved by the numerical integration of the state equation over the sampling time. The integration technique used here is the fourth order Runge-Kutta method [9]. The sampling time for updating the control input is determined by the pulse width that is modulated by the PWM generator.

V. Simulation Results of SCARA robot

Using the developed simulation package, the characteristics and performances of the SCARA are examined by changing payloads, control gains, and velocity profiles. A simulation is conducted on VAX/VMS 11-750 computer to perform the PTP (Point to Point) motion. A payload is 4 kg and a maximum speed is 3.5 m/sec. The current and velocity profiles are criteria for the analysis of the characteristics of the robot. The current must be within the rated current of motors and joint velocities must be accelerated and decelerated during the time periods determined in the trajectory plans. Based on these criteria, appropriate payloads, control gains, and velocities profiles are selected.

One of the simulation results is here demonstrated. Figure 5 shows the desired versus the actual position, velocity, and current at the first joint. The velocity is accelerated and reaches the maximum speed and is decelerated. The problem is the determination of the slope of the velocity curve. The simulation package can give the information for its selection based on the capacity of motor and manipulator dynamics. The current profile indicates the load acting on the motor. As shown in the figure, the current do not exceed the maximum limit specified by the manufacturer. The Figure 6 demonstrates the errors that occurred in the end of the robot arm. The SCARA has small position errors at the final position, which is less than 0.05 mm. In fact, the repeatability of the SCARA, which has been developed in CSIS, is close to 0.01 mm without payload.

VI. Conclusions

A fully integrated simulation package is developed for an industrial robot. A dynamic model is achieved by the combination of manipulator and actuator dynamics. A control is hard-ware oriented scheme and is the same as that of a SCARA robot. Simulation results present the effectiveness of various selective parameters and provide useful information in many aspects. However, the package has uncertainties in the dynamic model so that its results do not perfectly match to those of the real system. For improving the package, it is required to find uncertain factors by comparing the results of the simulation with those of the real system.

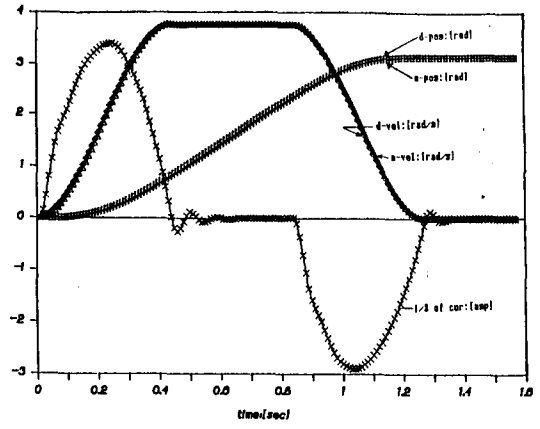

Figure 5. Desired versus Actual Position, Velocity, and Current Profiles.

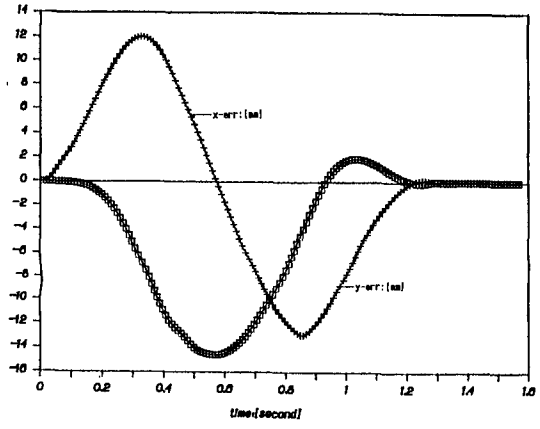

Figure 6. Position Errors of a Robot End-Effector in X and Y - Directions.

References

[1] Walker, M.W. and Orin, D.E.,"Efficient Dynamic Computer Simulation of Robotic Mechanisms," Trans. of ASME, Dynamic System, Measurement, and Control, Vol. 104, PP. 205-211, Sept. 1982

[2] Kankaanranta, R.K. and Koivo, H.N.,"Dynamics and Simulation of Compliant Motion of a Manipulator," IEEE Robotics and Automation, Vol. 4, No. 2, April 1988

[3] Luh, J.Y.S.,"An Anatomy of Industrial Robots, and Their Control," IEEE Trans. on Automatic Control, Vol. AC-28, No. 2, PP. 133-153, Feb. 1983

[4] Luh, J.Y.S.,"Conventional Controller Design for Industrial Robots - A Tutorial," IEEE Trans. on System, Man, and Cybernetics, Vol. SMC-13, No. 3, PP. 298-316, May/June 1983

[5] Craig, J.J., Introduction to Robotics: Mechanics and Control, Addison-Wesley Publishing Co., 1986

[6] Paul, R. P., Robot Manipulator : Methematics, Programming, and Control, M.I.T. Press, 1981

[7] Muir, P.F. and Neuman, C.P.,"Pulsewidth Modulation Control of Brushless DC Motors for Robotic Applications,"IEEE Trans. on Industrial Electronics, Vol.IE-32, No.3, PP. 222-229, Aug. 1985

[8] Hollerback, J.M.,"a Recursive Lagrangian Formulation of Manipulator Dynamics and a Comparative Study of Dynamics Formulation Complexity," IEEE Trans. on System, Man, and Cybernetics, Vol. 10, No. 11, PP. 730-736, Nov. 1980

[9] James, M.L., Smith, G.M., and Wolford, J.C., Applied Numerical Methods for Digital Computation, Happer & Row, Publishers, Inc., 1985